DOI: 10.1002/ejoc.200900743

Towards the Preparation of Electrochromic Materials with Strong Absorption in the Near-Infrared Region: Synthesis and Redox Behavior of Azulene-Substituted Enediyne Scaffolds Connected by a 9,10-Anthracenediyl Spacer

Shunji Ito,*[a] Takahiro Iida,[a] Jun Kawakami,[a] Tetsuo Okujima,[b] and Noboru Morita[c]

Keywords: Enynes / Cyanines / Carbanions / Redox chemistry / Electrochemistry

Enediyne scaffolds connected by a 9,10-anthracenediyl spacer as a redox-active substructure with 6-azulenyl groups as π-electron-accepting groups in their periphery (**3a** and **3b**) have been prepared by a one-pot reaction involving repeated Pd-catalyzed alkynylation of 6-haloazulenes **7b** and **7c** with bis(enediyne) derivative **6**. The azulene-substituted bis(enediyne)s **3a** and **3b** exhibited two reversible one-step, two-electron reduction properties upon cyclic voltammetry (CV) attributable to the formation of dianionic and tetraanionic species. The electrochemical reduction of **3a** and **3b** led a strong absorption in the near-IR region corresponding to the formation of the stabilized dianionic species $\mathbf{3a}_{RED}^{2-}$ and $\mathbf{3b}_{RED}^{2-}$. An electrochromic analysis revealed the lower stability of the tetraanionic species $\mathbf{3a}_{RED}^{4-\cdot\cdot}$ and $\mathbf{3b}_{RED}^{4-\cdot\cdot}$, although the CV exhibited good reversibility. The mono(enediyne) systems **11a** and **11b** were also prepared for comparison. The electrochemical reduction of **11a** and **11b** did not exhibit good electrochemical reversibility by CV, but the electrochemical reduction led to a strong absorption in the near-IR region, similar to the formation of the stabilized dianionic species $\mathbf{3a}_{RED}^{2-}$ and $3\mathbf{b}_{RED}^{2-}$ in the bis(enediyne) systems.

Introduction

Electrochromism is observed in reversible redox systems that exhibit significant color changes in different oxidation states.[1] The construction of organic molecules that contain multiple redox-active chromophores[2] is very important for the preparation of polyelectrochromic materials that respond to different potentials with a variety of colors.[3] The enediyne unit **1** is a molecular scaffold designed to facilitate the construction of one- and two-dimensional carbon networks (Figure 1).[4] Interest in conjugated enediyne systems has grown because of their wide range of applications, for example, in molecular wires, nonlinear optics (NLO), and molecular switches.

Electrochemical studies of enediyne systems have so far revealed their strong electron-accepting properties and a capacity for multi-electron reduction under cyclic voltammetric conditions.[5] Therefore we have tried to enhance the electron affinity and stability of the charged states of enediyne systems by introducing π-electron-accepting 6-azulenyl groups into the periphery. 9,10-Bis[bis(6-azulenylethynyl)methylene]-9,10-dihydroanthracenes **2a** and **2b** are an example of such enediyne systems with π-electron-accepting groups in their periphery. The anthraquinodimethane derivatives **2a** and **2b**, which possess a bis(enediyne) system with substantial redox stability, have been shown to exhibit one-step, two-electron reduction properties with a strong absorption in the near-infrared region in their dianionic states $\mathbf{2a}^{2+}$ (λ_{max} = 844 nm) and $\mathbf{2b}^{2+}$ (λ_{max} = 885 nm) (Figure 2).[6]

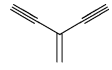

1

Figure 1. Enediyne scaffold **1**.

With a view to preparing electrochromic materials that exhibit strong absorption in the near-IR region under electrochemical reduction conditions, we have prepared the novel azulene-substituted enediyne scaffolds 9,10-bis[4-(6-azulenyl)-2-(6-azulenylethynyl)but-1-en-3-ynyl]anthracenes **3a** and **3b** in which the two enediyne units are located outside of the aromatic core. The electrochemical reduction of **3a** and **3b** produces an anthraquinodimethane substructure in addition to cyanine-type substructures in their two-electron reduced state. The formation of the anthraquinodimethane substructure might lead to an extension of their charge-transfer absorption band in the near-IR region in

[a] Graduate School of Science and Technology, Hirosaki University,
Hirosaki 036-8561, Japan
Fax: +81-172-39-3541
E-mail: itsnj@cc.hirosaki-u.ac.jp
[b] Department of Chemistry and Biology, Graduate School of Science and Engineering, Ehime University,
Matsuyama 790-8577, Japan
[c] Department of Chemistry, Graduate School of Science, Tohoku University,
Sendai 980-8578, Japan

Supporting information for this article is available on the WWW under http://dx.doi.org/10.1002/ejoc.200900743.

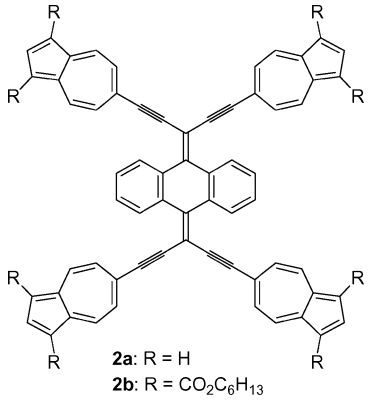

Figure 2. An enediyne system with π-electron-accepting 6-azulenyl groups in the periphery.

the two-electron reduced state. In this paper, we report the synthesis and electrochromic behavior of the novel azulene-substituted enediyne scaffolds **3a** and **3b** (Figure 3).

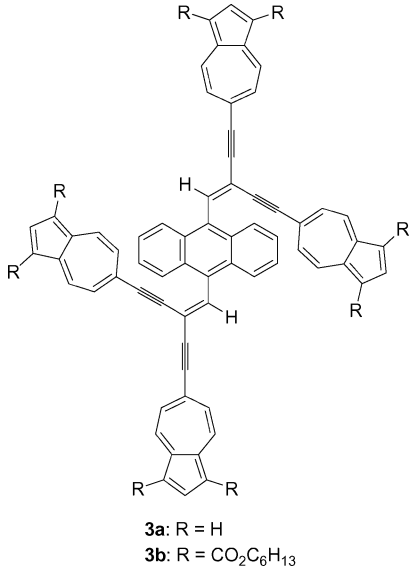

Figure 3. Novel azulene-substituted enediyne scaffolds **3a** and **3b**.

Results and Discussion

Synthesis

Azulene-substituted bis(enediyne) systems **3a** and **3b** were prepared by a simple one-pot reaction involving repeated Pd-catalyzed alkynylation of the bis(enediyne) scaffold **6**, prepared in solution via 9,10-bis[4-(trimethylsilyl)-2-[2-(trimethylsilyl)ethynyl]but-1-en-3-ynyl]anthracene (**5**), with 6-haloazulenes **7b** or **7c** under Sonogashira–Hagihara conditions (Scheme 1). The anthracene derivative **5** was prepared by the Pd-catalyzed alkynylation of 9,10-bis(2,2-dibromovinyl)anthracene (**4**)[7] with (trimethylsilyl)acetylene. The bis(enediyne) scaffold **6** was generated by the treatment of a solution of **5** in tetrahydrofuran with a methanolic potassium carbonate solution. The product **6** was stable enough in solution to be employed in the next transformation. The cross-coupling reaction of **6** with dihexyl 6-bromoazulene-1,3-diarboxylate (**7c**) using $[Pd(PPh_3)_4]$ as a catalyst and subsequent chromatographic purification of the reaction mixture on silica gel and gel permeation chromatography (GPC) afforded the desired **3b** in 42% yield. A similar reaction of **6** with 6-bromoazulene (**7a**) afforded **3a** in only 5% yield, probably due to the poorer reactivity of **7a** compared with **7c** and the instability of the enediyne core **6** under the reaction conditions. To improve the

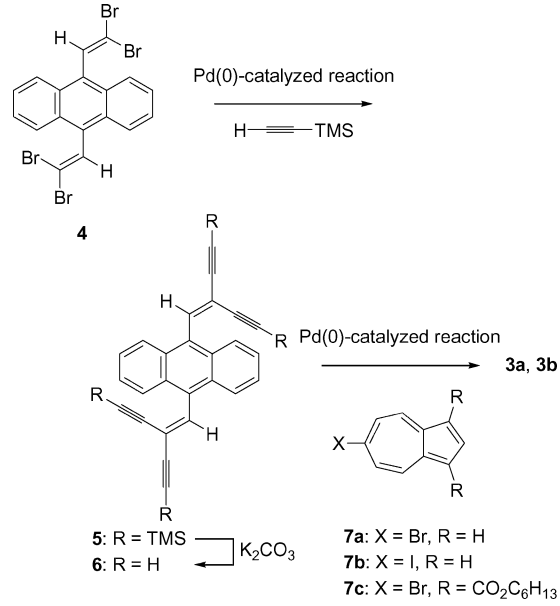

Scheme 1. Preparation of the novel azulene-substituted enediyne scaffolds **3a** and **3b**.

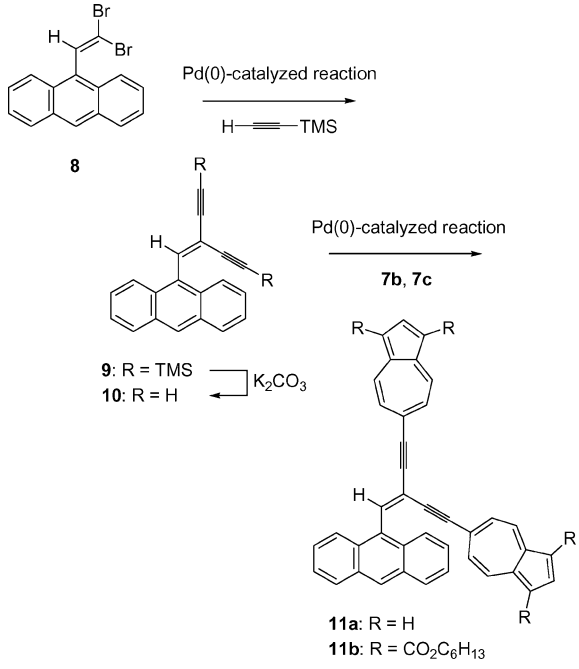

Scheme 2. Preparation of the mono(enediyne) derivatives **11a** and **11b**.

cross-coupling reaction, 6-iodoazulene (**7b**) was employed instead of **7a** to afford the desired bis(enediyne) compound **3a** in 54% yield (Scheme 1).

To confirm the effect of the bis(enediyne) structure in **3a** and **3b** we also prepared the mono(enediyne) derivatives **11a** and **11b** by using a cross-coupling procedure similar to that employed for the synthesis of **3a** and **3b** (Scheme 2). The Pd-catalyzed reaction of 1-(9-anthryl)-2-ethynylbut-1-en-3-yne (**10**), prepared in solution by the desilylation of 1-(9-anthryl)-4-(trimethylsilyl)-2-[2-(trimethylsilyl)ethynyl]-but-1-en-3-yne (**9**) with potassium carbonate in methanolic THF, with 6-haloazulenes **7b** and **7c** afforded the desired **11a** and **11b** in 72 and 59% yields, respectively.

Spectroscopic Properties

Compounds **3a**, **3b**, **11a**, and **11b** were fully characterized by spectroscopic methods (see the Exp. Sect.). The mass spectra of these compounds ionized by ESI showed the correct $[M + Na]^+$ ion peaks along with the $[M + K]^+$ and $[M + H]^+$ ion peaks in the case of the unsubstituted products **3a** and **11a** (R = H). The UV/Vis spectra of these compounds in dichloromethane are shown in Figures 4 and 5. In the electronic spectra, **3a** and **11a** exhibited weak absorptions in the visible region {**3a**: 622 nm [$\log\varepsilon$ = 3.24]; **11a**: 624 nm [$\log\varepsilon$ = 2.91]} characteristic of the azulene skeleton. However, **3b** and **11b** exhibited no clear characteristic weak absorption for the azulene derivatives in the long wavelength region, probably due to the overlapping of absorption bands {**3b**: 492 nm sh [$\log\varepsilon$ = 4.25]; **11b**: 490 nm sh [$\log\varepsilon$ = 3.87]} (Table 1). The absorption coefficients of the bis(enediyne)s **3a** and **3b** are almost twice as large as those of the mono(enediyne)s **11a** and **11b**. This indicates a small interaction between the two enediyne units in the bis(enediyne) systems **3a** and **3b**.

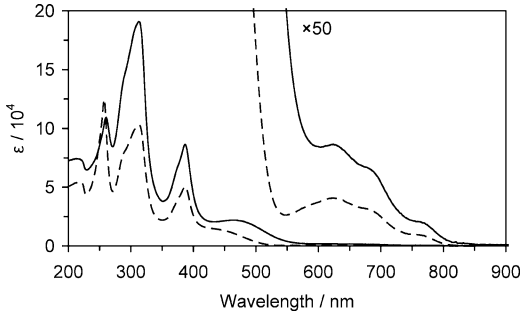

Figure 4. UV/Vis spectra of bis(enediyne) **3a** (solid line) and mono(enediyne) **11a** (broken line) in dichloromethane.

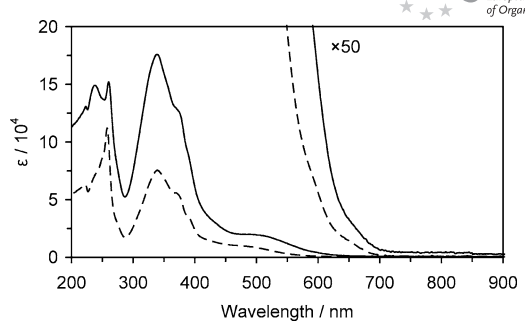

Figure 5. UV/Vis spectra of bis(enediyne) **3b** (solid line) and mono(enediyne) **11b** (broken line) in dichloromethane.

The azulene substituents facing the anthracene core in the bis(enediyne) systems **3a** and **3b** did not display sharp ^{1}H NMR signals at room temperature. Time-averaged ^{1}H NMR spectra were obtained by heating **3a** and **3b** in 1,1,2,2-[D_2]tetrachloroethane up to 80 °C. The temperature dependence of the ^{1}H NMR spectra of **3a** and **3b** was examined in $CDCl_3$ in the range of –60 to 50 °C. Selected ^{1}H NMR spectra of **3b** at various temperatures in $CDCl_3$ are shown in Figure 6 (a). The temperature dependence of the ^{1}H NMR spectra of **3a** and **3b** are shown in detail in the Supporting Information.

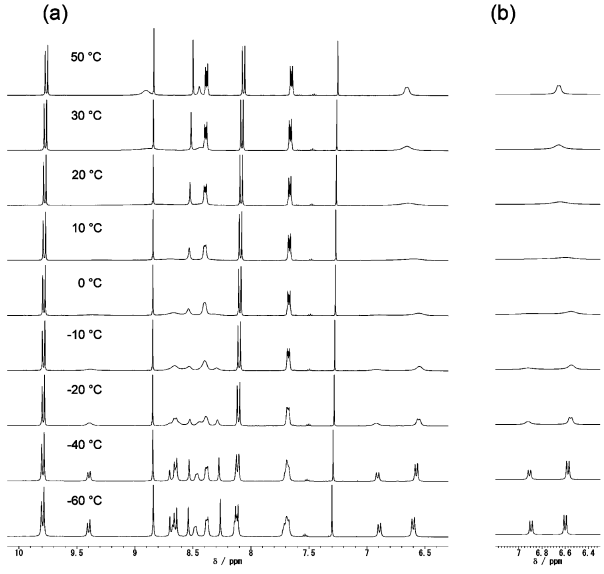

Figure 6. ^{1}H NMR (500 MHz) spectra of **3b** in $CDCl_3$ at various temperatures (–60, –40, –20, –10, 0, 10, 20, 30, and 50 °C, respectively, from the bottom): (a) aromatic region and (b) calculated spectra for the 6-azulenyl proton signals.

Table 1. Absorptions maxima and coefficients of **3a**, **3b**, **11a**, and **11b** in CH_2Cl_2.

	λ_{max} [nm] [$\log\varepsilon$]
3a	261 [5.04], 289 sh [5.16], 314 [5.28], 374 sh [4.82], 388 [4.94], 462 [4.34], 622 [3.24], 681 sh [3.12], 767 sh [2.59]
3b	238 [5.17], 260 [5.18], 339 [5.25], 373 sh [5.11], 492 sh [4.25]
11a	258 [5.10], 289 sh [4.90], 313 [5.01], 375 sh [4.60], 387 [4.70], 448 sh [4.13], 584 sh [2.84], 624 [2.91], 680 sh [2.80], 763 sh [2.27]
11b	238 sh [4.85], 249 sh [4.93], 258 [5.05], 340 [4.88], 369 [4.75], 389 sh [4.56], 490 sh [3.87]

The ^{1}H NMR spectrum of the bis(enediyne) derivative **3b** in $CDCl_3$ at –60 °C was observed to be frozen. At this temperature, the ^{1}H NMR spectrum consists of two 6-azulenyl signals arising from hydrogen atoms at the 5,7-positions in a ratio of around 1:1.4 at δ = 6.89 and 6.60 ppm, respectively. All the other signals also exhibited two sets of signals in a similar ratio to those of the 5,7-proton signals. When the sample was warmed to around 10 °C, noticeable line-broadening was observed and further warming resulted in the coalescence of the two signals.

The temperature dependency could be rationalized by the conformational isomerism of the *syn* and *anti* forms (**A** and **B**) in a propeller conformation, as illustrated in Figure 7. The large steric interaction among the 6-azulenyl substituents surrounding the central anthracene core in **3a** and **3b** would be responsible for the observation of the stereoisomerism revealed by the ^{1}H NMR spectra. The rate data determined by the line-shape analysis of the temperature-dependent ^{1}H NMR spectra of **3b** were used to calculate the free energies of activation for the stereoisomerization.[8]

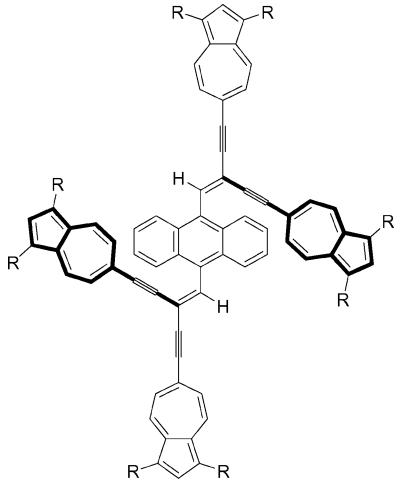

Figure 7. *syn*/*anti* forms (**A** and **B**) of **3a** and **3b** in a propeller conformation.

Selected results of the simulation analysis are shown in Figure 6 (b) and are summarized in detail in the Supporting Information. The barrier to the stereoisomerization ($\Delta G^{\neq}_{20}$) of the minor isomer to the major isomer of **3b** in $CDCl_3$ was calculated to be 54.1 ± 0.4 kJ mol^{-1} by the line-shape analysis.

The ^{1}H NMR spectrum of the bis(enediyne) system **3a** in $CDCl_3$ was also observed to be frozen at –60 °C. At this temperature, the ^{1}H NMR spectrum consists of two 6-azulenyl signals arising from the hydrogen atoms at the 5,7-positions in a ratio of around 1.8:1 at δ = 6.45 and 6.19 ppm, respectively, similar to the case of **3b**. The ^{1}H NMR spectra of **3a** also exhibited a similar temperature dependency to those of **3b** (see the Supporting Information). The barrier to the stereoisomerization ($\Delta G^{\neq}_{20}$) of the major isomer to the minor isomer of **3a** in $CDCl_3$ was calculated to be 52.1 ± 0.5 kJ mol^{-1} by a similar line-shape analysis. These results indicate that the ester substituents on the 6-azulenyl groups do not exert a significant influence on the stereoisomerization of **3a** and **3b**.

In contrast to the results obtained with **3a** and **3b**, the mono(enediyne) derivatives **11a** and **11b** exhibited well-resolved ^{1}H NMR spectra at room temperature. A variable-temperature ^{1}H NMR study of the mono(enediyne) derivative **11a** in $CDCl_3$ did not reveal any temperature dependency in the temperature range of –60 to 50 °C. These results are consistent with the results for the *syn* and *anti* isomerism of **3a** and **3b**.

Redox Potentials

The reduction potentials (E vs. $Ag/AgNO_3$) of **3a**, **3b**, **11a**, and **11b** measured by cyclic voltammetry (CV) and differential pulse voltammetry (DPV) are summarized in Table 2. The reduction waves of **3a**, **3b** and **11a**, **11b** measured by CV are presented in Figures 8 and 9, respectively. The oxidation potentials and the differential pulse voltammograms of these compounds are summarized in the Supporting Information. The voltammograms of **3a** and **3b** are characterized by two, one-step, two-electron reduction

Table 2. Reduction potentials of the compounds **3a**, **3b**, **11a**, and **11b**.[a]

		E_1^{red} [V]	E_2^{red} [V]
3a	E_{pa}	–1.21 (2e)	–1.92 (2e)
	E_{pc}	–0.91 (2e)	–1.66 (2e)
	E_{DPV}[b]	–1.09	–1.79
3b	E_{pa}	–1.07 (2e)	–1.48 (2e)
	E_{pc}	–0.62 (2e)	–1.29 (2e)
	E_{DPV}[b]	–0.94	–1.36
11a	E_{pa}	–1.51	–1.84
	E_{DPV}[b]	–1.42	–1.74
11b	E_{pa}	–1.24	–1.39
	E_{DPV}[b]	–1.13	–1.28

[a] The redox potentials [E vs. $Ag/AgNO_3$, E_{pa} (anodic peak potential) and E_{pc} (cathodic peak potential)] were measured by CV [1 mM in *o*-dichlorobenzene containing nBu$_4$NBF$_4$ (0.1 M), Pt electrode (i.d. 1.6 mm), scan rate 100 mV s^{-1}, and Fc/Fc^+ = +0.27 V]. [b] Peak potentials measured by DPV.

waves (Figure 8). The first cathodic peak corresponds to the reduction of **3a** and **3b** to the closed-shell dianions $\mathbf{3a}_{RED}^{2-}$ and $\mathbf{3b}_{RED}^{2-}$, respectively, by comparison with the results of the mono(enediyne) derivatives **11a** and **11b**. The second peak is ascribed to the formation of tetraanionic species such as $\mathbf{3a}_{RED}^{4-\bullet\bullet}$ and $\mathbf{3b}_{RED}^{4-\bullet\bullet}$ (Scheme 3). The less negative reduction potentials of **3b** compared with those of **3a** are attributable to the stabilization of the charged states by the hexyloxycarbonyl substituents. The two-electron reduction can be explained by the formation of a cyanine-type substructure in the dianionic forms $\mathbf{3a}_{RED}^{2-}$ and $\mathbf{3b}_{RED}^{2-}$, which should also generate a quinodimethane substructure in the central anthracene core.

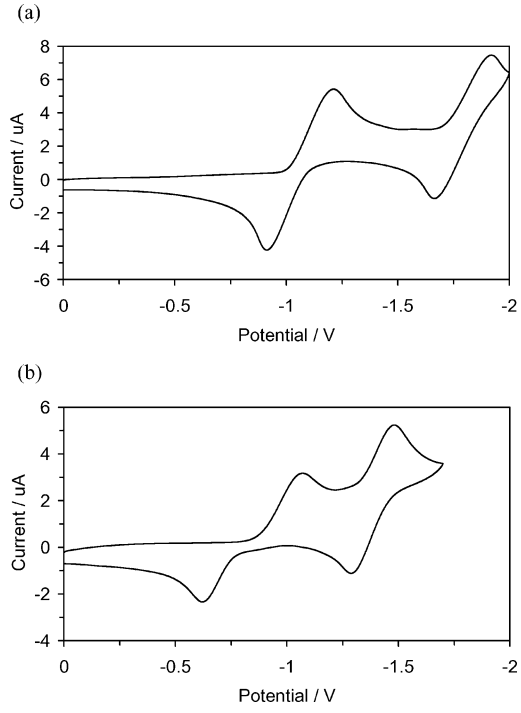

Figure 8. Cyclic voltammograms of (a) **3a** and (b) **3b** (1 mM) in *o*-dichlorobenzene containing $n\mathrm{Bu_4NBF_4}$ (0.1 M) as a supporting electrolyte.

The cyclic scan showed that the anodic peaks corresponding to the oxidation of $\mathbf{3a}_{RED}^{2-}$ and $\mathbf{3b}_{RED}^{2-}$ are positively shifted by 0.30 and 0.45 V, respectively, from the first cathodic peaks.[9] The positive shift of the anodic peaks in the first redox couple is consistent with the formation of the closed-shell dianions $\mathbf{3a}_{RED}^{2-}$ and $\mathbf{3b}_{RED}^{2-}$ in which the two enediyne moieties **3a** and **3b** are considered to adopt a twisted structure to release the steric interaction between the azulene rings and the central anthracene core. Some extra energy would be required to oxidize the twisted dianions back to the enediyne structures of neutral **3a** and **3b**. The positive shift in **3a** is slightly larger than that in **2a** (0.23 V). The hexyloxycarbonyl substituents are less effective in inducing the geometrical change in the electrochemical reduction of **3b** compared with **2b**, as indicated by the relatively small positive shift in **3b** compared with in **2b** (0.57 V). These results suggest that the conjugation between the two azulene rings is much more effective in the case of the two-electron reduction of **3b**, which should exhibit a considerable bathochromic shift in the two-electron reduced state $\mathbf{3b}_{RED}^{2-}$ compared with that in $\mathbf{2b}_{RED}^{2-}$.

The reduction potentials (E vs. $Ag/AgNO_3$) of the mono(enediyne)s **11a** and **11b** measured by CV are also summarized in Table 2. Figure 9 shows the reduction waves of **11a** and **11b** measured by CV. The electrochemical reduction of **11a** and **11b** exhibited two-step irreversible redox waves, which corresponds to the generation of dianionic species by two single-electron transfers (Scheme 4). Accordingly, these observations provide a criterion for the four-electron reduction of **3a** and **3b** in two steps. The first cathodic peak corresponds to the reduction of **11a** and **11b**, which are shifted more negatively by –0.30 and –0.17 V, respectively, compared with those for the reduction of **3a** and **3b**. These results are consistent with the stabilization of the dianionic

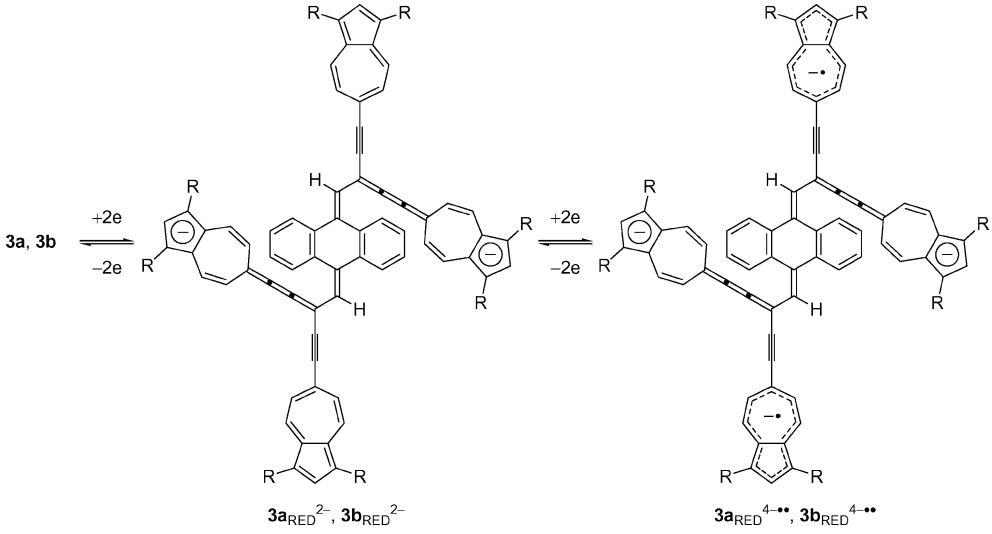

Scheme 3. Redox behavior of the novel azulene-substituted bis(enediyne) scaffolds **3a** and **3b**.

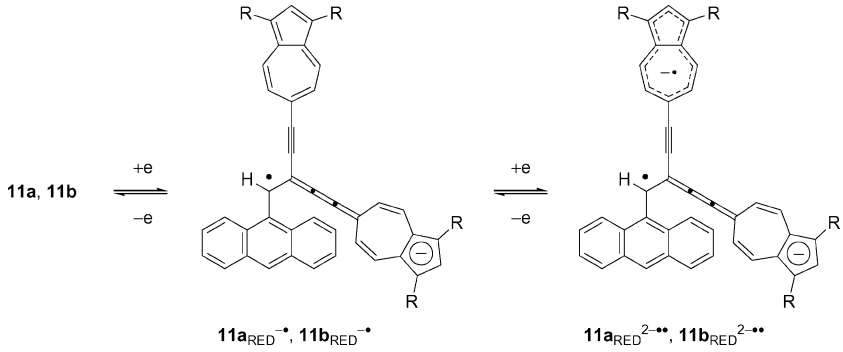

Scheme 4. Redox behavior of the mono(enediyne) derivatives **11a** and **11b**.

states by the formation a quinodimethane substructure in the central anthracene core in the two-electron reduction of **3a** and **3b**.

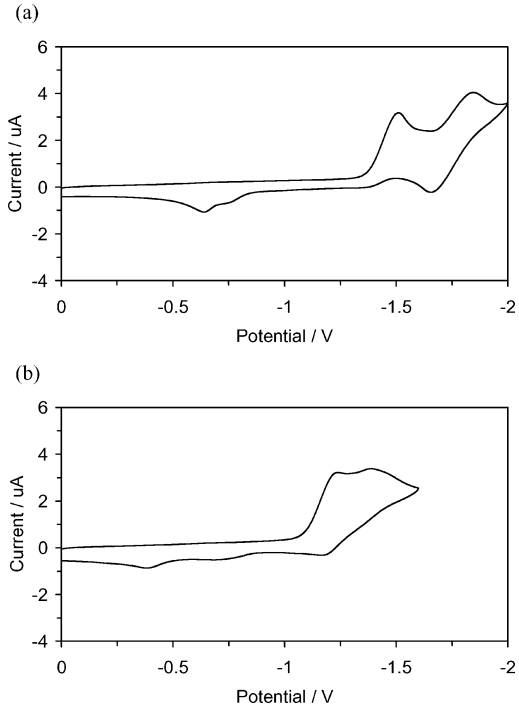

Figure 9. Cyclic voltammograms of (a) **11a** and (b) **11b** (1 mM) in *o*-dichlorobenzene containing nBu$_4$NBF$_4$ (0.1 M) as a supporting electrolyte.

trochemical reduction. The observed color change has been ascribed to the formation of a cyanine-type substructure in the two-electron reduction.

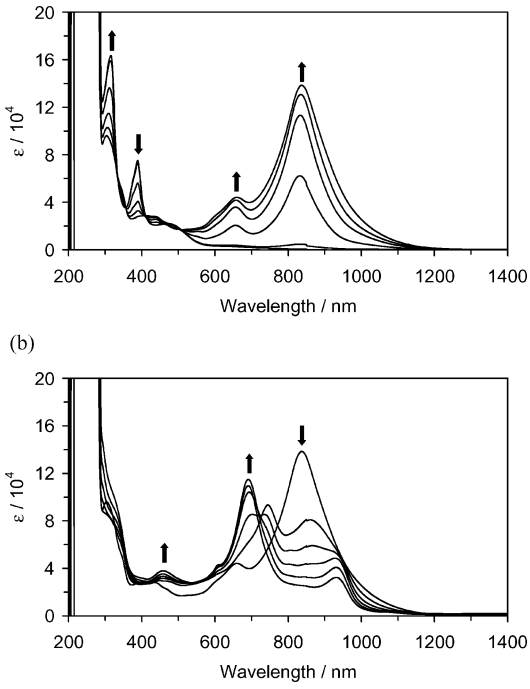

Figure 10. Continuous change in the UV/Vis spectrum of **3a** (2 mL; 9.00×10^{-5} M in 1 mm cell) in benzonitrile containing Et_4NClO_4 (0.1 M) upon (a) constant-current electrochemical reduction (100 μA) at 1.5 min intervals (**3a** → **3a**$_{RED}^{2-}$) and (b) further reduction of the green-colored solution at 19 min intervals.

Electrochromic Analysis

The electrochemical reduction of **3a**, **3b**, **11a**, and **11b** was monitored spectroscopically to clarify the formation of the colored species attributable to the formation of the dianions **3a**$_{RED}^{2-}$ and **3b**$_{RED}^{2-}$ with cyanine-type substructures. When the UV/Vis spectra of **3a** and **3b** were recorded under electrochemical reduction conditions in benzonitrile containing Et_4NClO_4 (0.1 M) at room temperature, a new absorption gradually developed in the near-IR region, as shown in parts a of Figures 10 and 11, respectively. Accordingly, the color of the solutions of **3a** (orange) and **3b** (orange) gradually changed to dark-green during the electrochemical reduction. The charge-transfer absorption bands in the spectra of **3a**$_{RED}^{2-}$ and **3b**$_{RED}^{2-}$ were observed as two bands from the visible region up to the near-IR region, although the electrochemical reduction of the anthraquinodimethane derivatives **2a** and **2b** exhibits one absorption band in these regions. This should be ascribed to the effect of the anthraquinodimethane substructure formed by the two-electron reduction, which should increase the electrochemical interaction of the two negative charged units. As suggested by the CV analysis, the longest absorption maxima of the hexyloxycarbonyl derivative **3b**$_{RED}^{2-}$ (λ_{max} = 799 and 967 nm) exhibits a considerable bathochromic shift in comparison with that of **2b**$_{RED}^{2-}$ (λ_{max} = 885 nm). In contrast, **3a**$_{RED}^{2-}$

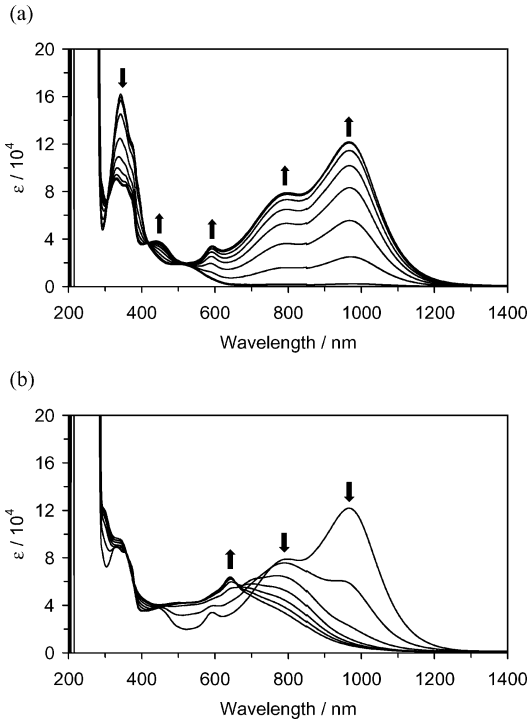

Figure 11. Continuous change in the UV/Vis spectrum of **3b** (2 mL; 1.19×10^{-4} M in 1 mm cell) in benzonitrile containing Et_4NClO_4 (0.1 M) upon (a) constant-current electrochemical reduction (100 μA) at 1 min intervals (**3b** → **3b**$_{RED}^{2-}$) and (b) further reduction of the green-colored species at 6 min intervals.

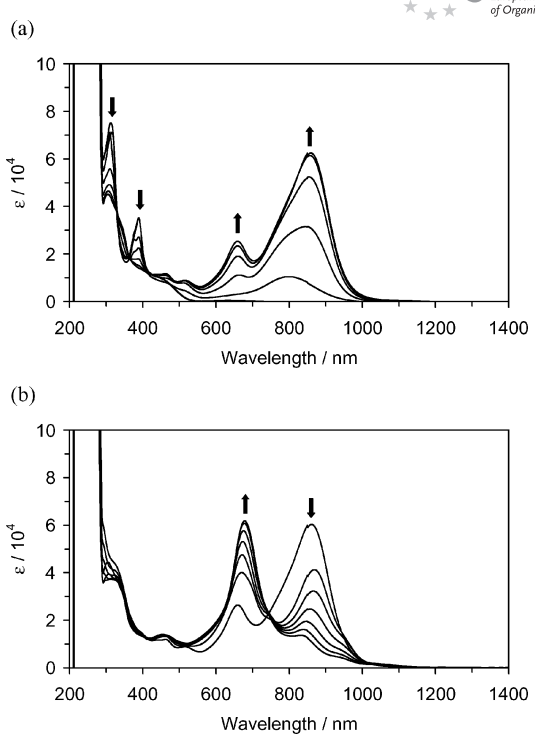

Figure 12. Continuous change in the UV/Vis spectrum of **11a** (2 mL; 1.35×10^{-4} M in a 1 mm cell) in benzonitrile containing Et_4NClO_4 (0.1 M) upon (a) constant-current electrochemical reduction (100 μA) at 2 min intervals and (b) further reduction of the green-colored species at 8 min intervals.

(λ_{max} = 658 and 837 nm) shows a slight hypsochromic shift of the longest absorption maxima, comparable with **2a**$_{RED}^{2-}$ (λ_{max} = 844 nm). These results indicate that the conjugation between the two azulene rings remains effective in the case of the two-electron reduction of **3b**, as suggested by the CV analysis. Reverse oxidation of the deeply colored solutions led to bleaching of the deep color to regenerate the UV/Vis spectra of the neutral **3a** and **3b** (see the Supporting Information).

On further reduction of the deeply colored solutions of **3a**$_{RED}^{2-}$ and **3b**$_{RED}^{2-}$, the new band in the near-IR region gradually decreased accompanied by an increment in two new absorption at 691 and 642 nm, respectively (see parts b in Figures 10 and 11). The dark-green color of the solutions changed to blue during the electrochemical reduction. However, the reverse oxidation of the blue-colored solutions did not regenerate the UV/Vis spectra of **3a**$_{RED}^{2-}$ and **3b**$_{RED}^{2-}$ with the dark-green color. The incomplete reversibility of the second reduction step suggests the instability of the tetraanionic species under the conditions of the UV/Vis spectral measurements, although good reversibility was observed upon CV.

We also monitored the electrochemical reduction of **11a** and **11b** by UV/Vis spectroscopy. The electrochemical reduction of **11a** and **11b** should form the radical-anionic species **11a**$_{RED}^{\cdot-}$ and **11b**$_{RED}^{\cdot-}$ during the redox reaction. The electrochemical reduction afforded new absorption bands in the near-IR region (**11a**: λ_{max} = 661 and 865 nm; **11b**: λ_{max} = 663 and 908 nm; see parts a in Figures 12 and 13), similar

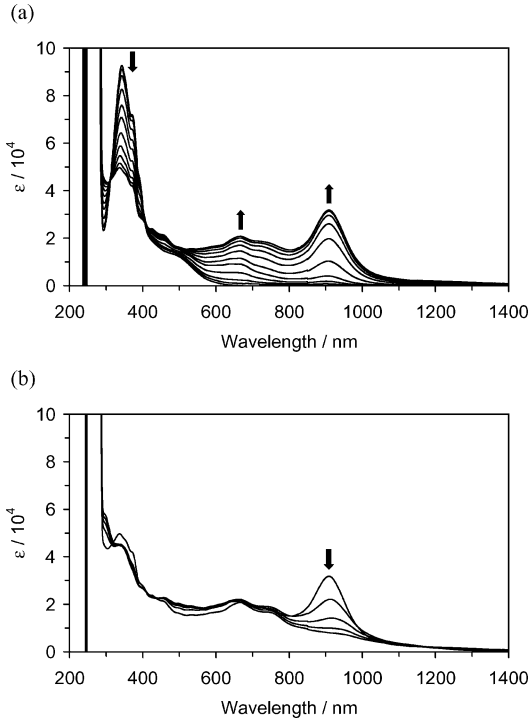

Figure 13. Continuous change in the UV/Vis spectrum of **11b** (2 mL; 2.07×10^{-4} M in a 1 mm cell) in benzonitrile containing Et_4NClO_4 (0.1 M) upon (a) constant-current electrochemical reduction (100 μA) at 1 min intervals and (b) further reduction of the green-colored species at 6 min intervals.

to those of the bis(enediyne)s **3a** and **3b**, although the CV analysis revealed the poor reversibility for the redox reaction. On further reduction of the deeply colored solutions, the new band in the near-IR region gradually decreased accompanied by an increment in a new absorption at 699 and 644 nm, respectively (parts b in Figures 12 and 13). The dark-green color of the solutions changed to light-blue during the electrochemical reduction. The incomplete reversibility of the UV/Vis spectral changes is consistent with the results of the CV analyses, which suggest the instability of the anionic species in **11a** and **11b** under the electrochemical conditions.

Conclusions

Enediyne scaffolds connected by a 9,10-anthracenediyl spacer as a redox-active substructure with 6-azulenyl groups as π-electron-accepting groups in their periphery have been synthesized. The bis(enediyne) systems **3a** and **3b** can be assumed to be a violene–cyanine hybrid, a concept proposed by Hünig and co-workers for the design of stabilized organic electrochromic materials.[10] From the viewpoint of generating an anthraquinodimethane substructure in addition to the formation of cyanine-type substructures by two-electron reduction, these bis(enediyne) systems **3a** and **3b** are examples of the hybrid system composed of an inverse Wurster-type violene core. Their presumed two, one-step, two-electron reduction properties with substantial redox stability was revealed by CV analyses, which suggests that the ester substituents on the 6-azulenyl groups do not appreciably contribute to geometrical changes in the electrochemical reduction compared with the anthraquinodimethane derivatives **2a** and **2b**. An electrochromic analysis revealed that the conjugation between the two azulene rings remains much more effective in the case of the two-electron reduction of the ester derivative **3b**, which resulted in the development of a broad absorption up to the near-IR region in the two-electron reduced state $\mathbf{3b}_{RED}^{2-}$. Construction of stabilized polyelectrochromic systems utilizing the enediyne scaffold to respond to multi-electron reduction will be a focus of our future work.

Experimental Section

General: For general and electrochemical measurement details, see the Supporting Information. The assignment of peaks in the ^1H and ^{13}C NMR spectra was achieved by H–H COSY, NOE, HMQC, and/or HMBC experiments.

9,10-Bis[4-(6-azulenyl)-2-(6-azulenylethynyl)but-1-en-3-ynyl]anthracene (3a): K_2CO_3 (146 mg, 1.06 mmol) was added to a solution of **5** (295 mg, 0.480 mmol) in THF (30 mL), MeOH (90 mL), and water (0.9 mL). The resulting mixture was stirred at room temperature for 3 h. After the addition of diethyl ether (200 mL) and water (100 mL) to the reaction mixture, the organic layer was separated, washed with water, dried with $MgSO_4$, and concentrated under reduced pressure until around 50 mL. Compound **7b** (933 mg, 3.67 mmol), CuI (46 mg, 0.24 mmol), triethylamine (60 mL), and THF (60 mL) were added to the solution. [$Pd(PPh_3)_4$] (66 mg, 0.057 mmol) was added to the degassed mixture and the mixture was stirred at room temperature for 5 h. The reaction mixture was then diluted with CH_2Cl_2, washed successively with 5% NH_4Cl and brine, dried with $MgSO_4$, and concentrated under reduced pressure. The residue was purified by column chromatography on silica gel with hexane/dichloromethane (1:1) to afford **3a** (215 mg, 54%) and the recovered **7b** (404 mg, 43%). Brown needles; m.p. 210 °C (decomp.; hexane). IR (KBr disk): $\tilde{\nu}_{max}$ = 3079 (w), 3013 (w), 2198 (w, C≡C), 1571 (s), 1541 (m), 1468 (w), 1445 (m), 1395 (s), 1353 (w), 1296 (w), 1266 (w), 1216 (w), 1190 (w), 1043 (w), 965 (w), 837 (s), 821 (m), 670 (w), 753 (s), 732 (m), 698 (w), 643 (w), 605 (w), 566 (w), 452 (w), 430 (w) cm^{-1}. UV/Vis (CH_2Cl_2): λ_{max} = 261 [logε = 5.04], 289 sh [5.16], 314 [5.28], 374 sh [4.82], 388 [4.94], 462 [4.34], 622 [3.24], 681 sh [3.12], 767 sh [2.59] nm. ^1H NMR [500 MHz, $(CDCl_2)_2$, 80 °C]: δ = 8.37–8.34 (m, 4 H, 1,4,5,8-H), 8.30 (s, 2 H, 1′-H), 8.28 (d, $^3J_{H,H}$ = 10.3 Hz, 4 H, 4‴,8‴-H), 7.90 (t, $^3J_{H,H}$ = 3.7 Hz, 2 H, 2‴-H), 7.66 (t, $^3J_{H,H}$ = 3.7 Hz, 2 H, 2⁗-H), 7.65 (d, $^3J_{H,H}$ = 10.2 Hz, 4 H, 4⁗,8⁗-H), 7.59–7.56 (m, 4 H, 2,3,6,7-H), 7.54 (d, $^3J_{H,H}$ = 10.3 Hz, 4 H, 5‴,7‴-H), 7.40 (d, $^3J_{H,H}$ = 3.7 Hz, 4 H, 1‴,3‴-H), 7.05 (d, $^3J_{H,H}$ = 3.7 Hz, 4 H, 1⁗,3⁗-H), 6.29 (d, $^3J_{H,H}$ = 10.2 Hz, 4 H, 5⁗,7⁗-H) ppm. ^{13}C NMR [125 MHz, $(CDCl_2)_2$, 80 °C]: δ = 144.41 (C-1′), 140.31 (C-3‴a,8‴a), 139.85 (C-3⁗a,8⁗a), 138.41 (C-2‴), 137.96 (C-2⁗), 135.24 (C-4‴,8‴), 134.52 (C-4⁗,8⁗), 131.76 (C-6‴), 131.64 (C-9,10), 130.83 (C-6⁗), 129.40 (C-4a,8a,9a,10a), 126.98 (C-1,4,5,8), 126.42 (C-2,3,6,7,5‴,7‴), 125.66 (C-5⁗,7⁗), 119.68 (C-1‴,3‴), 119.19 (C-1⁗,3⁗), 111.34 (C-2′), 99.48 (C-2″), 94.06 (C-4′), 90.19 (C-3′ or C-1″), 88.52 (C-3′ or C-1″) ppm. MS (ESI positive): *m*/*z* (%) = 869 (12) $[M + K]^+$, 853 (100) $[M + Na]^+$, 831 (12) $[M + H]^+$. HRMS: calcd. for $C_{66}H_{38} + K^+$ 869.2605; found 869.2603. HRMS: calcd. for $C_{66}H_{38} + Na^+$ 853.2866; found 853.2864. HRMS: calcd. for $C_{66}H_{38} + H^+$ 831.3046; found 831.3047. $C_{66}H_{38}\cdot{}^2/_3H_2O$ (831.01): calcd. C 94.03, H 4.70; found C 93.98, H 5.14.

9,10-Bis{4-[1,3-bis(hexyloxycarbonyl)-6-azulenyl]-2-[1,3-bis(hexyloxycarbonyl)-6-azulenylethynyl]but-1-en-3-ynyl}anthracene (3b): K_2CO_3 (80 mg, 0.58 mmol) was added to a solution of **5** (150 mg, 0.244 mmol) in THF (20 mL), MeOH (45 mL), and water (0.5 mL). The resulting mixture was stirred at room temperature for 3 h. After the addition of diethyl ether (200 mL) and water (100 mL) to the reaction mixture, the organic layer was separated, washed with water, dried with $MgSO_4$, and concentrated under reduced pressure until around 40 mL. Compound **7c** (910 mg, 1.96 mmol), CuI (22 mg, 0.12 mmol), triethylamine (35 mL), and THF (40 mL) was added to the solution. [$Pd(PPh_3)_4$] (38 mg, 0.033 mmol) was added to the degassed mixture, which was stirred at room temperature for 5 h. The reaction mixture was diluted with CH_2Cl_2, washed successively with 5% NH_4Cl and brine, dried with $MgSO_4$, and concentrated under reduced pressure. The residue was purified by column chromatography on silica gel with hexane/dichloromethane (1:3) and GPC with chloroform to afford **3b** (189 mg, 42%) and the recovered **7c** (449 mg, 49%). Reddish-brown crystals; m.p. 201.2–202.6 °C (hexane). IR (KBr disk): $\tilde{\nu}_{max}$ = 3045 (w), 2955 (s), 2929 (s), 2857 (m), 2203 (w, C≡C), 1695 (s, C=O), 1580 (m), 1567 (m), 1542 (m), 1510 (w), 1466 (w), 1431 (s), 1400 (m), 1364 (w), 1296 (w), 1233 (m), 1199 (s), 1101 (w), 1074 (m), 1041 (w), 1018 (m), 906 (w), 853 (m), 800 (w), 762 (m), 734 (w), 654 (w) cm^{-1}. UV/Vis (CH_2Cl_2): λ_{max} = 238 [logε 5.17], 260 [5.18], 339 [5.25], 373 sh

[5.11], 492 sh [4.25] nm. ^{1}H NMR [500 MHz, $(CDCl_2)_2$, 80 °C]: δ = 9.68 (d, $^3J_{H,H}$ = 11.0 Hz, 4 H, 4‴,8‴-H), 8.88 (d, $^3J_{H,H}$ = 10.3 Hz, 4 H, 4⁗,8⁗-H), 8.78 (s, 2 H, 2‴-H), 8.46 (s, 2 H, 1′-H), 8.42 (s, 2 H, 2⁗-H), 8.36–8.33 (m, 4 H, 1,4,5,8-H), 8.03 (d, $^3J_{H,H}$ = 11.0 Hz, 4 H, 5‴,7‴-H), 7.63–7.60 (m, 4 H, 2,3,6,7-H), 6.66 (d, $^3J_{H,H}$ = 10.3 Hz, 4 H, 5⁗,7⁗-H), 4.36 (t, $^3J_{H,H}$ = 6.7 Hz, 8 H, Hex-1-H), 4.25 (t, $^3J_{H,H}$ = 6.7 Hz, 8 H, Hex-1′-H), 1.81 (tt, $^3J_{H,H}$ = 7.5, 6.7 Hz, 8 H, Hex-2-H), 1.75 (tt, $^3J_{H,H}$ = 7.4, 6.8 Hz, 8 H, Hex-2′-H), 1.48 (m, 8 H, Hex-3-H), 1.42 (m, 8 H, Hex-3′-H), 1.38–1.29 (m, 16 H, Hex-4,5,4′,5′-H), 0.90 (t, $^3J_{H,H}$ = 7.0 Hz, 12 H, Hex-6-H or Hex-6′-H), 0.87 (t, $^3J_{H,H}$ = 7.2 Hz, 12 H, Hex-6-H or Hex-6′-H) ppm. ^{13}C NMR [125 MHz, $(CDCl_2)_2$, 80 °C]: δ = 165.01 (1‴,3‴-CO_2Hex), 164.54 (1⁗,3⁗-CO_2Hex), 147.09 (C-1′), 144.46 (C-2‴), 143.96 (C-2⁗), 143.63 (C-3‴a,8‴a), 142.89 (C-3⁗a,8⁗a), 137.86 (C-4‴,8‴), 136.84 (C-4⁗,8⁗), 135.60 (C-6‴), 134.37 (C-6⁗), 133.45 (C-5‴,7‴), 132.53 (C-5⁗,7⁗), 131.54 (C-9,10), 129.28 (C-4a,8a,9a,10a), 126.88 (C-1,4,5,8 or C-2,3,6,7), 126.83 (C-1,4,5,8 or C-2,3,6,7), 118.02 (C-1‴,3‴), 117.42 (C-1⁗,3⁗), 110.81 (C-2′), 98.09 (C-2″), 93.18 (C-4′), 92.51 (C-3′ or C-1″), 90.89 (C-3′ or C-1″), 64.84 (Hex-C-1), 64.63 (Hex-C-1′), 31.73 (Hex-C-4,4′), 29.18 (Hex-C-2), 29.12 (Hex-C-2′), 26.05 (Hex-C-3), 26.01 (Hex-C-3′), 22.76 (Hex-C-5 or Hex-C-5′), 22.73 (Hex-C-5 or Hex-C-5′), 14.18 (Hex-C-6 or Hex-C-6′), 14.17 (Hex-C-6 or Hex-C-6′) ppm. MS (ESI positive): *m/z* (%) = 1878 (73) [M + Na]$^+$. HRMS: calcd. for $C_{122}H_{134}O_{16}$ + Na$^+$ 1877.9564; found 1877.9570. $C_{122}H_{134}O_{16}$ (1856.36): calcd. C 78.93, H 7.28; found C 78.87, H 7.41.

9,10-Bis[4-(trimethylsilyl)-2-[2-(trimethylsilyl)ethynyl]but-1-en-3-ynyl]anthracene (5): $[PdCl_2(PPh_3)_2]$ (652 mg, 0.929 mmol) was added to a solution of **4** (2.50 g, 4.58 mmol), (trimethylsilyl)acetylene (5.40 g, 55.0 mmol), and CuI (357 mg, 1.87 mmol) in Et_3N (125 mL). The resulting mixture was stirred at 50 °C for 4 h under Ar. The reaction mixture was diluted with toluene, washed successively with 5% NH_4Cl and brine, dried with $MgSO_4$, and concentrated under reduced pressure. The residue was purified by column chromatography on silica gel with hexane/toluene (1:1) and GPC with chloroform to afford **5** (619 mg, 22%). Yellow prisms; m.p. 207.9–209.2 °C (hexane). IR (KBr disk): $\tilde{\nu}_{max}$ = 3096 (w), 3017 (w), 2958 (m), 2881 (w), 2154 (m, C≡C), 1440 (w), 1407 (w), 1372 (w), 1327 (w), 1250 (m), 1179 (m), 1030 (m), 914 (m), 899 (m), 845 (s), 755 (m), 730 (w), 694 (w), 645 (w), 370 (w) cm^{-1}. UV/Vis (CH_2Cl_2): λ_{max} = 223 [logε = 4.56], 254 [4.85], 269 sh [4.73], 309 [4.06], 321 [4.08], 424 [4.21] nm. ^{1}H NMR (500 MHz, $CDCl_3$): δ = 8.17–8.13 (m, 4 H, 1,4,5,8-H), 8.04 (s, 2 H, 1′-H), 7.51–7.47 (m, 4 H, 2,3,6,7-H), 0.31 (s, 18 H, TMS), –0.38 (s, 18 H, TMS) ppm. ^{13}C NMR (125 MHz, $CDCl_3$): δ = 144.41 (C-1′), 130.61 (C-9,10), 128.65 (C-4a,8a,9a,10a), 126.72 (C-1,4,5,8), 125.35 (C-2,3,6,7), 110.79 (C-2′, C-3′, or C-1″), 102.55 (C-2′, C-3′, or C-1″), 100.71 (C-2′, C-3′, or C-1″), 100.56 (C-4′ or C-2″), 94.10 (C-4′ or C-2″), –0.10 [TMS (^{1}H = 0.31)], –0.87 [TMS (^{1}H = –0.38)] ppm. $C_{38}H_{46}Si_4$ (615.11): calcd. C 74.20, H 7.54; found C 73.94, H 7.72.

1-(9-Anthryl)-4-(trimethylsilyl)-2-[2-(trimethylsilyl)ethynyl]but-1-en-3-yne (9): $[PdCl_2(PPh_3)_2]$ (750 mg, 1.07 mmol) was added to a solution of **8** (2.83 g, 7.82 mmol),[11] (trimethylsilyl)acetylene (4.77 g, 48.6 mmol), and CuI (403 mg, 2.12 mmol) in Et_3N (140 mL). The resulting mixture was stirred at 50 °C for 4 h under Ar. The reaction mixture was diluted with toluene, washed successively with 5% NH_4Cl and brine, dried with $MgSO_4$, and concentrated under reduced pressure. The residue was purified by column chromatography on silica gel with hexane/toluene (1:1) and GPC with chloroform to afford **9** (1.01 g, 33%). Yellow prisms; m.p. 110.3–111.6 °C (hexane). IR (KBr disk): $\tilde{\nu}_{max}$ = 3096 (w), 3051 (w), 3017 (w), 2959 (m), 2896 (w), 2155 (m, C≡C), 1617 (w), 1519 (w), 1444 (w), 1409 (w), 1352 (w), 1330 (w), 1307 (w), 1249 (s), 1188 (m), 1177 (m), 1156 (w), 1138 (w), 1067 (w), 1015 (w), 954 (w), 934 (w), 907 (s), 893 (m), 875 (m), 845 (s), 789 (w), 760 (s), 732 (s), 700 (w), 677 (w), 641 (w), 623 (w), 609 (w), 546 (w), 410 (w) cm^{-1}. UV/Vis (CH_2Cl_2): λ_{max} = 224 [logε 4.42], 253 sh [4.91], 257 [4.92], 301 [3.70], 314 [3.65], 349 sh [3.58], 368 sh [3.83], 395 [4.01] nm. ^{1}H NMR (500 MHz, $CDCl_3$): δ = 8.42 (s, 1 H, 10-H), 8.13 (s, $^3J_{H,H}$ = 9.7 Hz, 2 H, 1,8-H), 8.05 (s, 1 H, 1′-H), 7.99 (d, $^3J_{H,H}$ = 9.6 Hz, 2 H, 4,5-H), 7.50–7.44 (m, 4 H, 2,3,6,7-H), 0.31 (s, 9 H, TMS), –0.37 (s, 9 H, TMS) ppm. ^{13}C NMR (125 MHz, $CDCl_3$): δ = 144.33 (C-1′), 131.16 (C-4a,10a), 129.41 (C-9), 129.19 (C-8a,9a), 128.61 (C-4,5), 127.82 (C-10), 126.42 (C-1,8), 125.56 (C-2,7), 125.16 (C-3,6), 110.55 (C-2′, C-3′, or C-1″), 102.62 (C-2′, C-3′, or C-1″), 100.86 (C-2′, C-3′, or C-1″), 100.49 (C-4′ or C-2″), 93.96 (C-4′ or C-2″), –0.09 [TMS (^{1}H = 0.31)], –0.92 [TMS (^{1}H = –0.37)] ppm. $C_{26}H_{28}Si_2$ (396.67): calcd. C 78.72, H 7.11; found C 78.79, H 7.21.

1-(9-Anthryl)-4-(6-azulenyl)-2-[2-(6-azulenyl)ethynyl]but-1-en-3-yne (11a): K_2CO_3 (144 mg, 1.04 mmol) was added to a solution of **10** (178 mg, 0.449 mmol) in THF (28 mL), MeOH (85 mL), and water (0.7 mL). The resulting mixture was stirred at room temperature for 3 h. After the addition of diethyl ether (200 mL) and water (100 mL) to the reaction mixture, the organic layer was separated, washed with water, dried with $MgSO_4$, and concentrated under reduced pressure until around 40 mL. Compound **7b** (432 mg, 1.70 mmol), CuI (51 mg, 0.27 mmol), triethylamine (55 mL), and THF (55 mL) were added to the solution. $[Pd(PPh_3)_4]$ (67 mg, 0.058 mmol) was added to the degassed mixture, which was stirred at room temperature for 6 h. The reaction mixture was diluted with CH_2Cl_2, washed successively with 5% NH_4Cl and brine, dried with $MgSO_4$, and concentrated under reduced pressure. The residue was purified by column chromatography on silica gel with hexane/dichloromethane (2:1) to afford **11a** (162 mg, 72%) and further purification by column chromatography on silica gel with hexane afforded the recovered **7b** (252 mg, 58%). Green prisms; m.p. 190 °C (decomp.; hexane). IR (KBr disk): $\tilde{\nu}_{max}$ = 3068 (w), 3034 (w), 3005 (w), 2199 (w, C≡C), 1571 (s), 1541 (m), 1471 (w), 1443 (w), 1396 (s), 1361 (w), 1219 (w), 1193 (w), 1046 (w), 1008 (w), 969 (w), 888 (w), 839 (s), 823 (w), 784 (w), 753 (m), 732 (s), 604 (w), 565 (w) cm^{-1}. UV/Vis (CH_2Cl_2): λ_{max} = 258 [logε 5.10], 289 sh [4.90], 313 [5.01], 375 sh [4.60], 387 [4.70], 448 sh [4.13], 584 sh [2.84], 624 [2.91], 680 sh [2.80], 763 sh [2.27] nm. ^{1}H NMR (500 MHz, $CDCl_3$): δ = 8.53 (s, 1 H, 10-H), 8.31 (d, $^3J_{H,H}$ = 10.4 Hz, 2 H, 4‴,8‴-H), 8.31 (s, 1 H, 1′-H), 8.29 (d, $^3J_{H,H}$ = 8.6 Hz, 2 H, 1,8-H), 8.07 (d, $^3J_{H,H}$ = 9.1 Hz, 2 H, 4,5-H), 7.93 (t, $^3J_{H,H}$ = 3.7 Hz, 1 H, 3‴-H), 7.91 (d, $^3J_{H,H}$ = 10.5 Hz, 2 H, 4⁗,8⁗-H), 7.78 (t, $^3J_{H,H}$ = 3.7 Hz, 1 H, 3⁗-H), 7.54–7.49 (m, 4 H, 2,3,6,7-H), 7.54 (d, $^3J_{H,H}$ = 10.4 Hz, 2 H, 5‴,7‴-H), 7.43 (d, $^3J_{H,H}$ = 3.7 Hz, 2 H, 1‴,3‴-H), 7.23 (d, $^3J_{H,H}$ = 3.7 Hz, 2 H, 1‴,3‴-H), 6.44 (d, $^3J_{H,H}$ = 10.5 Hz, 2 H, 5⁗,7⁗-H) ppm. ^{13}C NMR (125 MHz, $CDCl_3$): δ = 144.33 (C-1′), 139.92 (C-3‴a,8‴a), 139.65 (C-3⁗a,8⁗a), 138.05 (C-3‴), 137.78 (C-3⁗), 135.03 (C-4‴,8‴), 134.54 (C-4⁗,8⁗), 131.47 (C-6‴), 131.28 (C-4a,10a), 130.96 (C-6⁗), 129.37 (C-9a, C-2′, or C-8a,9a), 129.31 (C-9a, C-2′, or C-8a,9a), 129.86 (C-4,5), 128.49 (C-10), 126.19 (C-1,8), 126.13 (C-2,7 or C-5‴,7‴), 126.07 (C-2,7 or C-5‴,7‴), 125.55 (C-5⁗,7⁗), 125.41 (C-3,6), 119.22 (C-1‴,3‴), 118.77 (C-1⁗,3⁗), 110.14 (C-9 or C-2′), 98.98 (C-2″), 93.46 (C-4′), 89.75 (C-3′ or C-1″), 88.43 (C-3′ or C-1″) ppm. MS (ESI positive): *m/z* (%) = 543 (3.8) [M + K]$^+$, 527 (100) [M + Na]$^+$, 505 (8) [M + H]$^+$. HRMS: calcd. for $C_{40}H_{24}$ + K$^+$ 543.1510; found 543.1511. HRMS: calcd. for $C_{40}H_{24}$ + Na$^+$ 527.1770; found 527.1768. HRMS: calcd. for $C_{40}H_{24}$ + H$^+$ 505.1951; found 505.1953. $C_{40}H_{24}\cdot^1/_3H_2O$ (504.61): calcd. C 94.09, H 4.87; found C 93.98, H 5.29.

1-(9-Anthryl)-4-[1,3-bis(hexyloxycarbonyl)-6-azulenyl]-2-{2-[1,3-bis-(hexyloxycarbonyl)-6-azulenyl}ethynyl}but-1-en-3-yne (11b): K_2CO_3 (141 mg, 1.02 mmol) was added to a solution of **10** (181 mg, 0.456 mmol) in THF (30 mL), MeOH (85 mL), and water (0.7 mL). The resulting mixture was stirred at room temperature for 3 h. After the addition of diethyl ether (200 mL) and water (100 mL) to the reaction mixture, the organic layer was separated, washed with water, dried with $MgSO_4$, and concentrated under reduced pressure until around 50 mL. Compound **7c** (842 mg, 1.82 mmol), CuI (33 mg, 0.17 mmol), triethylamine (58 mL), and THF (60 mL) were added to the solution. [$Pd(PPh_3)_4$] (63 mg, 0.055 mmol) was added to the degassed mixture and the mixture was stirred at room temperature for 5 h. The reaction mixture was diluted with CH_2Cl_2, washed successively with 5% NH_4Cl and brine, dried with $MgSO_4$, and concentrated under reduced pressure. The residue was purified by column chromatography on silica gel with hexane/dichloromethane (1:1) and dichloromethane to afford **12b** (274 mg, 59%) and the recovered **7c** (446 mg, 53%). Dark-brown prisms; m.p. 128.6–129.9 °C (hexane). IR (KBr disk): $\tilde{\nu}_{max}$ = 3045 (w), 2955 (s), 2930 (s), 2858 (m), 2202 (w, C≡C), 1695 (s, C=O), 1580 (m), 1567 (w), 1542 (w), 1509 (w), 1466 (w), 1431 (s), 1390 (m), 1365 (w), 1256 (w), 1234 (w), 1200 (s), 1104 (w), 1075 (m), 1018 (m), 907 (w), 890 (w), 854 (m), 787 (w), 763 (w), 733 (m), 656 (w), 609 (w) cm^{-1}. UV/Vis (CH_2Cl_2): λ_{max} = 238 sh [log ε 4.85], 249 sh [4.93], 258 [5.05], 340 [4.88], 369 [4.75], 389 sh [4.56], 490 sh [3.87] nm. ^{1}H NMR (500 MHz, $CDCl_3$): δ = 9.74 (d, $^3J_{H,H}$ = 11.1 Hz, 2 H, 4‴,8‴-H), 9.33 (d, $^3J_{H,H}$ = 11.1 Hz, 2 H, 4⁗,8⁗-H), 8.82 (s, 1 H, 2‴-H), 8.68 (s, 1 H, 2⁗-H), 8.57 (s, 1 H, 10-H), 8.49 (s, 1 H, 1′-H), 8.27 (d, $^3J_{H,H}$ = 8.5 Hz, 2 H, 1,8-H), 8.11 (d, $^3J_{H,H}$ = 9.1 Hz, 2 H, 4,5-H), 8.03 (d, $^3J_{H,H}$ = 11.1 Hz, 2 H, 5‴,7‴-H), 7.59–7.53 (m, 4 H, 2,3,6,7-H), 6.90 (d, $^3J_{H,H}$ = 11.1 Hz, 2 H, 5⁗,7⁗-H), 4.40 (t, $^3J_{H,H}$ = 6.7 Hz, 4 H, Hex-1-H), 4.33 (t, $^3J_{H,H}$ = 6.7 Hz, 4 H, Hex-1′-H), 1.85 (t, $^3J_{H,H}$ = 7.6, 6.7 Hz, 4 H, Hex-2-H), 1.79 (t, $^3J_{H,H}$ = 7.5, 6.7 Hz, 4 H, Hex-2′-H), 1.52 (m, 4 H, Hex-3-H), 1.47 (m, 4 H, Hex-3′-H), 1.42–1.33 (m, 8 H, Hex-4,5,4′,5′-H), 0.94 (t, $^3J_{H,H}$ = 7.1 Hz, 6 H, Hex-6-H or Hex-6′-H), 0.91 (t, $^3J_{H,H}$ = 7.0 Hz, 6 H, Hex-6-H or Hex-6′-H) ppm. ^{13}C NMR (125 MHz, $CDCl_3$): δ = 164.92 (1‴,3‴-CO_2Hex), 164.82 (1⁗,3⁗-CO_2Hex), 147.24 (C-1′), 144.02 (C-2‴), 143.78 (C-2⁗), 143.50 (C-3‴a,8‴a), 143.31 (C-3⁗a,8⁗a), 137.57 (C-4‴,8‴), 137.08 (C-4⁗,8⁗), 135.30 (C-6‴), 134.81 (C-6⁗), 133.22 (C-5‴,7‴), 132.74 (C-5⁗,7⁗), 131.24 (C-4a,10a or C-8a,9a), 129.23 (C-4a,10a or C-8a,9a), 129.19 (C-10), 129.10 (C-4,5), 128.66 (C-9), 126.47 (C-2,7), 125.87 (C-1,8), 125.55 (C-3,6), 117.29 (C-1‴,3‴), 116.87 (C-1⁗,3⁗), 109.18 (C-2′), 97.82 (C-2″), 92.49 (C-4′), 92.30 (C-3′ or C-1″), 91.03 (C-3′ or C-1″), 64.46 (Hex-C-1), 64.34 (Hex-C-1′), 31.52 (Hex-C-4 or Hex-C-4′), 31.48 (Hex-C-4 or Hex-C-4′), 28.85 (Hex-C-2), 28.79 (Hex-C-2′), 25.82 (Hex-C-3), 25.77 (Hex-C-3′), 22.57 (Hex-C-5 or Hex-C-5′), 22.55 (Hex-C-5 or Hex-C-5′), 14.03 (Hex-C-6 or Hex-C-6′), 14.01 (Hex-C-6 or Hex-C-6′) ppm. MS (ESI positive): *m*/*z* = 1040 (100) [M + Na]$^+$. HRMS: calcd. for $C_{68}H_{72}O_8$ + Na^+ 1039.5119; found 1039.5114. $C_{68}H_{72}O_8$ (1017.29): calcd. C 80.28, H 7.13; found C 80.22, H 7.28.

Supporting Information (see also the footnote on the first page of this article): General and experimental details of the electrochemical measurements, variable-temperature NMR results for **3a** and **3b**, voltammograms and spectroelectrograms of **3a**, **3b**, **11a**, and **11b**, ^{1}H and ^{13}C NMR spectra of **3a**, **3b**, **5**, **9**, **11a**, and **11b**.

Acknowledgments

This work was supported by the Ministry of Education, Culture, Sports, Science, and Technology, Japan by a Grant-in-Aid for Scientific Research (Grant 18550026 to S. I.).

[1] P. M. S. Monk, R. J. Mortimer, D. R. Rosseinsky, *Electrochromism*: *Fundamentals and Applications*, VCH, Weinheim, **1995**.
[2] K. Deuchert, S. Hünig, *Angew. Chem.* **1978**, *90*, 927–938; *Angew. Chem. Int. Ed. Engl.* **1978**, *17*, 875–886.
[3] a) T. Komatsu, K. Ohta, T. Fujimoto, I. Yamamoto, *J. Mater. Chem.* **1994**, *4*, 533–536; b) D. R. Rosseinsky, D. M. S. Monk, *J. Appl. Electrochem.* **1994**, *24*, 1213–1221.
[4] For example, see: a) H. Hopf, J. Kämpen, P. Bubenitschek, P. G. Jones, *Eur. J. Org. Chem.* **2002**, 1708–1721; b) M. B. Nielsen, F. Diederich, *Synlett* **2002**, 544–552; c) F. Diederich, *Chem. Commun.* **2001**, 219–227; d) F. Diederich, *Pure Appl. Chem.* **1999**, *71*, 265–273.
[5] J. Anthony, A. M. Boldi, C. Boudon, J.-P. Gisselbrecht, M. Gross, P. Seiler, C. B. Knobler, F. Diederich, *Helv. Chim. Acta* **1995**, *78*, 797–817.
[6] S. Ito, H. Inabe, N. Morita, A. Tajiri, *Eur. J. Org. Chem.* **2004**, 1774–1780.
[7] G. T. Hwang, H. S. Son, J. K. Ku, B. H. Kim, *J. Am. Chem. Soc.* **2003**, *125*, 11241–11248.
[8] The rate data were determined by utilizing the chemical exchange simulation program produced by Prof. Hiroshi Nakamura of Hokkaido University.
[9] The peak separation of a ferrocenium/ferrocene (Fc^+/Fc) couple was 0.25 V under the conditions of the CV measurements.
[10] a) S. Hünig, M. Kemmer, H. Wenner, I. F. Perepichka, P. Bäuerle, A. Emge, G. Gescheid, *Chem. Eur. J.* **1999**, *5*, 1969–1973; b) S. Hünig, M. Kemmer, H. Wenner, F. Barbosa, G. Gescheidt, I. F. Perepichka, P. Bäuerle, A. Emge, K. Peters, *Chem. Eur. J.* **2000**, *6*, 2618–2632; c) S. Hünig, I. F. Perepichka, M. Kemmer, H. Wenner, P. Bäuerle, A. Emge, *Tetrahedron* **2000**, *56*, 4203–4211; d) S. Hünig, A. Langels, M. Schmittel, H. Wenner, I. F. Perepichka, K. Peters, *Eur. J. Org. Chem.* **2001**, 1393–1399.
[11] T. R. Kelly, J. P. Sestelo, I. Tellitu, *J. Org. Chem.* **1998**, *63*, 3655–3665.

Received: July 6, 2009
Published Online: September 18, 2009

